**Proceedings of ASME 2026
International Mechanical Engineering Congress and Exposition
IMECE-INDIA2026
September, 03-05, 2026, Chennai, India**

IMECE-INDIA2026-187891

ON SYNCHRONIZATION OF SIMILAR AND DISSIMILAR MECHANICAL SYSTEMS VIA INDIRECT VIBRATIONAL COUPLING

Anubhab Sinha
Institute of Engineering
and Management,
University of Engineering
and Management,
Kolkata, India
sinhaanubhab@gmail.com

Anirban Mondal
Institute of Engineering
and Management,
University of Engineering and
Management,
Kolkata, India
anirbanmondal2003@gmail.com

Aritra Das
Institute of Engineering
and Management,
University of Engineering
and Management,
Kolkata, India
aritradas803@gmail.com

Sayan Mandal
Institute of Engineering
and Management,
University of Engineering
and Management,
Kolkata, India
sayanmandalbankadaha@gmail.com

ABSTRACT

The present work examines cooperative dynamics in mechanically independent systems, each driven by its own DC motor. Interaction occurs solely through indirect vibrational pathways, without any kinematic linkage, allowing both structurally similar and dissimilar mechanisms to participate in a shared dynamical environment. Three representative configurations are considered. The first involves two cam–follower systems interacting through an intermediate mass excited by their follower motions. The second introduces configurational asymmetry by replacing one cam-follower with a scotch–yoke mechanism, with coupling again mediated through base excitation of the intermediate element. The third extends the interaction to a shared vibrating base structure supporting a slider–crank mechanism and an eccentric disk rotor, enabling energy exchange through the support structure. In a broader sense, synchronization in mechanical systems is examined through two complementary viewpoints. One concerns passive vibrational synchronization, arising from base excitation, while the other pertains to synchronization under active excitation generated by reciprocating and rotating unbalances. The criteria for the emergence of in-phase and ant-phase synchronization are investigated using multi-body dynamic simulations in MSC Adams, with particular attention given to the role of resonance and the nature of excitation. The results suggest that coordinated behavior can arise as a self-organized response to vibrational coupling, even under pronounced differences in power input and configuration asymmetry, pointing toward a generalized route to synchronization in distributed mechanical systems.

Keywords: Synchronization; Vibrational coupling; Cam–follower mechanism; Scotch–yoke mechanism; Slider–crank mechanism; unbalanced disk rotor system

1. INTRODUCTION

In recent years, there has been growing interest in how mechanical systems can behave collectively, especially through synchronization, where independent systems gradually adjust their motion and begin to operate in a coordinated way. Traditionally, such coordination is achieved using direct mechanical connections like gears, shafts, or belts, or through centralized control. However, many real engineering systems operate without these connections, which naturally raises the question of how coordination can still emerge under such conditions.

One possible explanation lies in vibration. Mechanical systems inherently generate vibrations due to moving parts and periodic excitations, and these vibrations can travel through supporting structures or intermediate elements. In doing so, they create pathways for energy exchange between otherwise independent systems. This allows systems to influence each other and develop coordinated motion without any direct linkage. Importantly, such a type of behavior is not limited to identical systems, but it can also happen between structurally different kinds of mechanisms, which is often the case in real applications.

The previous work provided on synchronization mainly focuses on identical systems [1,7,9,12]. These complete studies found that vibration could serve as a medium for interaction, even when no direct stiffness-based connection actually exists [9,10]. They also proved that synchronization mainly depends on factors such as frequency of excitation, coupling strength, and phase relationships [3,4]. However, this emphasis on identical systems limits the applications of these findings to more realistic situations where systems are often different in design and operation point of view.

More recent research has started to consider the effects of nonlinearity, asymmetry, and system-level dynamics, showing that synchronization can still occur through indirect interactions such as base vibrations or compliant elements [3,5,8]. Even so, most studies remain restricted to similar systems under simplified conditions, leaving a gap in understanding how dissimilar, independently driven systems behave when coupled through vibrations [7].

It is the main gap this work features. The focus falls mainly on synchronization arising from vibrational energy exchange between mechanically independent systems having its own DC motor each, covering both similar and dissimilar mechanisms that interact only through indirect vibrational pathways. Two main interaction types are considered: one where coupling happens through an intermediate element driven by motion of the base, and another where a shared vibrating structure hosts mechanisms with both reciprocating and rotating imbalances. In neither case are the systems kinematically connected — their relationship is purely dynamic, mediated by mechanical vibration.

Looking at these configurations brings the study close enough to real engineering conditions and paints a fuller picture of how synchronization actually works. It shows that coordinated motion can arise naturally through energy exchange, even when systems are structurally very different. That's a useful starting point for thinking about how to design distributed mechanical systems where direct connections aren't an option.

2. DYNAMICAL SETUPS

Two distinct dynamical configurations are examined, each defined by how excitation arises and how the systems interact:

Case I: Passive excitation.

Here, two independently motor-driven subsystems — referred to as system #1 and system #2 — interact by inducing motion in a shared intermediate structure, as shown in Fig. 1. The excitation isn't built into the structure itself; it comes from the kinematic output of the subsystems acting on it from either side. In the first version of this setup, both subsystems are cycloidal cam–follower mechanisms, one on the left and one on the right of the intermediate vibrating block. The block gets shaken by the motion of both followers pushing on it from opposite sides. In the second version, one of the cam–follower systems is replaced by a scotch–yoke mechanism. The block is still excited from both sides - the follower on the left, the yoke on the right - but now the two subsystems are structurally different from each other, thus introducing an asymmetry while the overall mode of excitation stays passive.

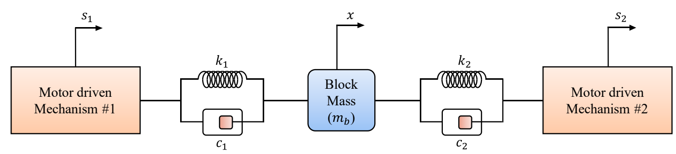

FIG. 1. SCHEMATIC OF PASSIVE EXCITATION MODELS (CASE I)

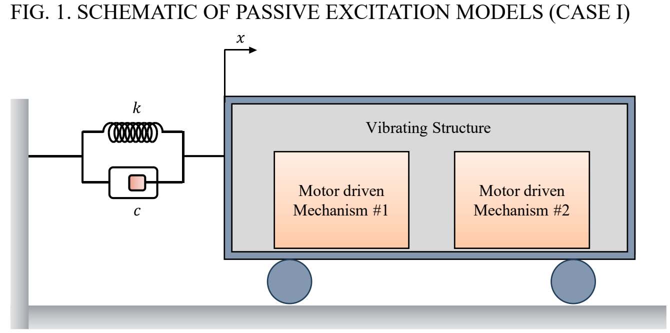

FIG. 2. SCHEMATIC OF ACTIVE EXCITATION MODELS (CASE II)

Case II: Active excitation.

In the following configuration, the vibrating base directly puts on the two independently driven mechanisms in such a way that the excitation comes from within, i.e., from the dynamical imbalance of the mechanisms themselves, rather than being imposed on from outside. The setup shown in Fig. 2. A slider–crank mechanism (SCM) serves as system #1, and an eccentric disk rotor (EDR) serves as system #2. The Slider Crank Mechanism generates both rotating and reciprocating unbalances, while the Eccentric Disc Rotor contributes mainly in the rotational imbalance. Together all of these unbalances keep the base in sustained motion which thereby creates a fundamentally different kind of interaction compared to the passive case.

Across all configurations, each system is driven by a DC motor treated as non-ideal - meaning it has a finite power supply and its behavior is shaped by the mechanical load it's driving. Rather than prescribing a fixed motion, the motor interacts dynamically with the system. Its output torque is modeled using a non-ideal DC motor formulation –

$$T_m = \frac{k_m V_s - k_m^2 \omega_m}{R_m} \quad (1)$$

where T_m denotes the electromagnetic torque generated by the motor, k_m is the motor constant characterizing the electromechanical coupling, V_s represents the applied supply voltage, R_m is the angular velocity of the motor shaft, and is the armature resistance governing the electrical dynamics.

3. Case I - PASSIVE EXCITATION MODELS

As mentioned, we will take up two separate setups to study the passively base excited synchronization models (refer Fig. 1).

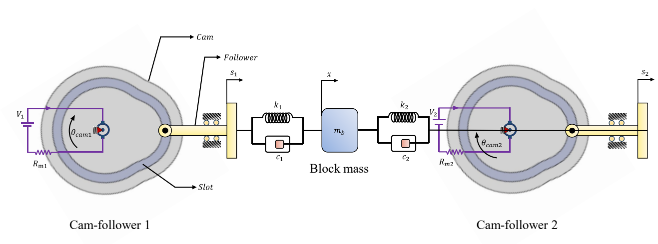

FIG. 3. SCHEMATIC OF PASSIVE EXCITATION MODEL WITH TWO CAM FOLLOWER SYSTEMS (CASE I (a))

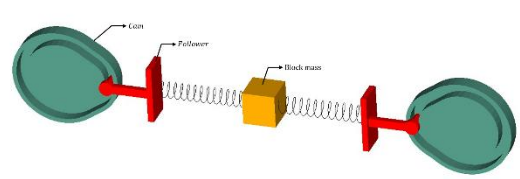

FIG. 4. ADAMS MODEL OF CAM-CAM SETUP (CASE I (a))

3.1 Case I (a) - Cam-cam Model

In the first setup of case I, the mechanical system consists of two cam-follower mechanisms, as shown in Figure 1. These mechanisms are positioned on either side of an Intermediate vibrating block. The systems use cycloidal slotted cam-follower design, as referenced in earlier work [13]. This specific arrangement is intentionally selected so that the follower act as source of base excitation to the block (see Fig. 3). As a result, there is no direct mechanical connection between the two-cam system. Due to this, any interaction between the two cams occurs only through the intermediate vibrating mass. The detailed terminology and parameter value used for this cam-cam configuration are provided in Table 1.

A corresponding multibody representation of the system is implemented in MSC Adams (Fig. 4), using the parameters provided in Table 1 for numerical simulation. The system's dynamic behavior is then analyzed under various combinations of input voltages supplied to the motors that drive the cams. This study aims to investigate whether the two subsystems can synchronize by exchanging energy through the intermediate vibrating block alone.

Table 1. Nomenclature and modelling parameters – Case I (a)

Components	Symbol	Description	Value
Motor #1	V_1	Voltage supply	-
	k_{m1}	Characteristic constant	0.5 Nm/A
	R_{m1}	Circuit resistance	0.4 Ω
Motor #2	V_2	Voltage supply	-
	k_{m2}	Characteristic constant	0.5 Nm/A
	R_{m2}	Circuit resistance	0.4 Ω
System #1 Cam-Follower 1	J_{cam1}	Combined Rotary inertia (motor 1 & cam 1)	0.25 kg-m^2
	M_{f1}	Follower 1 mass	0.5 kg
	s_1	Follower 1 displacement	-
	θ_{cam1}	Cam 1 angular displacement	-
	ω_{cam1}	Cam 1 angular speed	-
	β_1	Ascent/Descent angle	1.2 rad
	H_1	Lift height	0.09 m
System #2 Cam-Follower 2	J_{cam2}	Combined Rotary inertia (motor 2 & cam 2)	0.25 kg-m^2
	M_{f2}	Follower 2 mass	0.5 kg
	s_2	Follower 2 displacement	-
	θ_{cam2}	Cam 2 angular displacement	-
	ω_{cam2}	Cam 2 angular speed	-
	β_2	Ascent/Descent angle	1.2 rad
	H_2	Lift height	0.09 m
	k_c	Contact stiffness	1e8 N/m
	c_c	Contact damping	100 Ns/m

Miscellaneous	m_b	Block Mass	2 kg
	x	Block displacement	-
	k_1	Spring stiffness 1	10000 N/m
	c_1	Viscous damping 1	50 Ns/m
	k_2	Spring stiffness 2	10000 N/m
	c_2	Viscous damping 2	50 Ns/m
	Ω_1	Natural frequency of model (case I)	100 rad/s

The theoretical natural frequency (Ω_1) of the system (see Table 1) is about 100 rad/s ($= ((k_1 + k_2)/m_b)$, whereas the motor characteristics suggest steady-state RMS speeds of approximately 110 rad/s (55 V) and 132 rad/s (62 V). However, as observed in Fig. 5(a), both cams converge to a synchronized speed of nearly 84 rad/s. Although this value does not exactly match the theoretical natural frequency, the value is sufficiently near the natural frequency implies that resonance is influencing the system response. This shift from the ideal resonance point can be attributed to the influence of non-ideal motor characteristics, since higher power is required to achieve true resonance.

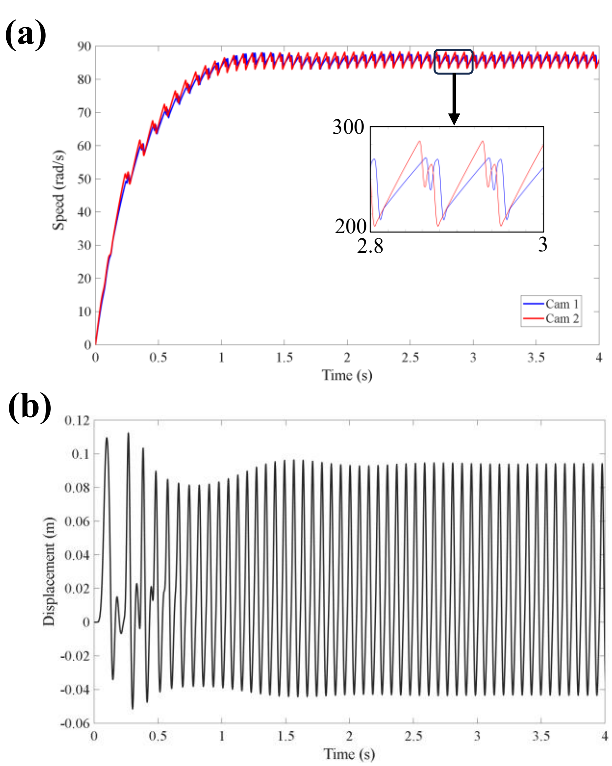

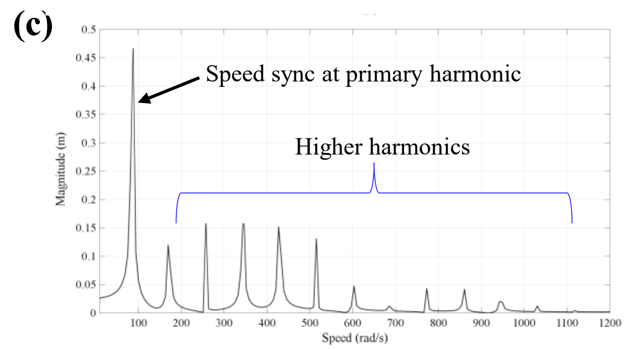

FIG. 5. IN-PHASE SYNC AT $V_1 = 55\,V, V_2 = 62\,V$, (a) SPEED RESPONSE OF BOTH CAMS, (b) DISPLACEMENT OF BLOCK MASS, (c) FFT OF DISPLACEMENT RESPONSE AT STEADY STATE.

Furthermore, the large amplitude oscillation of the intermediate block, shown in Fig. 5(b), plays an important role in synchronization process. Since the two cam systems are not connected through any direct mechanical linkage, the intermediate block serves as the only medium through which interaction and energy transfer between two cam systems can occur. As the vibration amplitude of the block increases, the exchange of energy between two cam systems becomes stronger, which eventually helps the systems to evolve towards synchronized motion.

Further evidence of this behaviour can be observed from the frequency-domain (FFT) analysis of the block displacement shown in Fig. 5(c). A strong peak appears at the primary harmonic corresponding to the resonance-locked speed (i.e. 84 rad/sec), indicating that synchronization is established near this resonance-linked frequency. In addition to the dominant peak, several higher-order harmonics are also present in the spectrum. These arise due to cycloidal motion of cam profile, which naturally produces frequency components at multiples of the fundamental excitation frequency, resulting in a multi-frequency response of the system.

Although the nominal natural frequency of the system is 100 rad/s, synchronization is observed at approximately 84 rad/s due to resonance capture associated with the Sommerfeld Effect [13]. As the excitation frequency approaches the natural frequency, vibration amplitudes increase progressively, and the system enters the resonance zone before the exact resonant condition is reached. For the present motor power input, stable operation occurs at 84 rad/s, where sufficiently strong vibration-induced coupling promotes in-phase synchronization. With higher motor voltage, the synchronized speed would shift closer to the natural frequency.

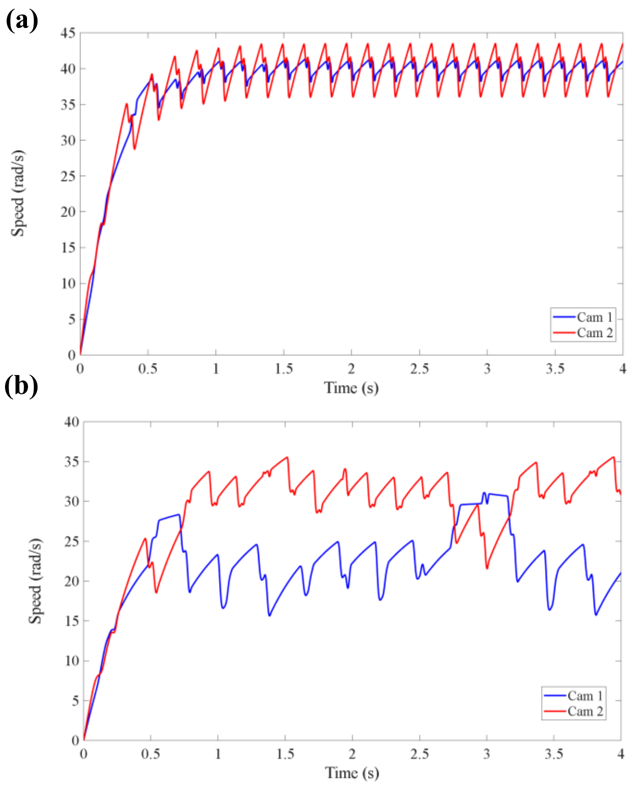

FIG. 6. SPEED RESPONSE - (a) IN-PHASE SYNC AT $V_1 = 24\,V, V_2 = 34V$, (b) TENDENCY TO SYNC AT $V_1 = 15\,V, V_2 = 20V$

Although the primary harmonic mainly governs the overall system behaviours because of its much larger magnitude, the higher-order harmonics continue to exist with smaller amplitudes and may contribute to secondary resonance interactions. Such characteristics are typical of cycloidal cam profile systems and have also been discussed in [13]. Even though the influence of these higher harmonics is relatively weak, their presence enhances the dynamic response of the system and creates additional possibilities for weaker synchronization behaviour to occur.

This behaviour can be clearly observed in Fig. 6(a) and (b). Figure 6(a) shows that, for the 24 V–34 V input condition, the system achieves speed synchronization at a frequency close to half of the natural frequency (i.e. $\Omega_1 / 2$), The synchronized frequency is observed near 41 rad/s, while the corresponding theoretical value is approximately 50 rad/s.

As expected, synchronization in this subharmonic region is weaker compared to that near the primary resonance. In contrast, Fig. 6(b), corresponding to the 16 V–20 V input combination, shows only a partial tendency toward synchronization near one-third of the natural frequency (i.e. $\Omega_1 / 3$) (with a theoretical value of approximately 33.3 rad/s). In this regime, nonlinearities disrupt the system's ability to achieve stable phase synchronization. However, the system still displays a noticeable inclination toward synchronization, as seen from the repeated crossing of the motor speed curves, suggesting intermittent coordination without achieving sustained locking.

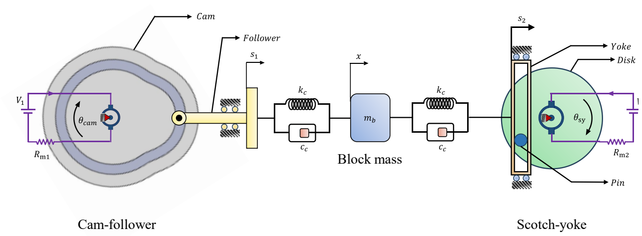

FIG. 7. SCHEMATIC OF PASSIVE EXCITATION MODEL WITH CAM FOLLOWER & SCOTCH-YOKE SYSTEMS (CASE I (b))

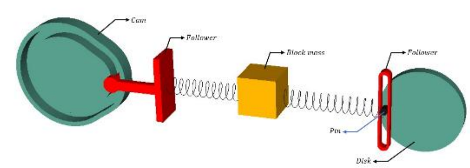

FIG. 8. ADAMS MODEL OF CAM-SCOTCH-YOKE SETUP (CASE I (b))

3.2 Case I (b) - Cam scotch-yoke model

In the second setup corresponding to Case I, one of the cam–follower subsystems is replaced with a scotch–yoke mechanism, while the other cam–follower unit is kept unchanged. These two subsystems are positioned on either side of the intermediate vibrating block, with the follower acting on one side and the yoke on the other, as shown in Fig. 7. Under this arrangement, the block experience base excitation rom cam-follower and scotch-yoke mechanism. Although this arrangement introduces configurational asymmetry, the two subsystems remain indirectly coupled, with no direct kinematic linkage between them.

All parameters related to Motor 1, Motor 2, and the remaining system components are kept the same as those listed in Table 1. Changes are introduced only in the cam–follower and scotch–yoke subsystems, for which the relevant geometric and kinematic parameters are provided separately in Table 2. The corresponding multibody dynamic model developed in MSC Adams is presented in Fig. 8.

Table 2. Nomenclature and modelling parameters – Case I (b)

Components	**Symbol**	**Description**	**Value**
System #1 Cam-Follower	J_{cam}	Combined Rotary inertia (motor & cam)	0.05 kg-m^2
	M_f	Follower mass	0.5 kg
	s_1	Follower displacement	-
	θ_{cam}	Cam angular displacement	-
	ω_{cam}	Cam angular speed	-
	β	Ascent/Descent angle	1 rad
	H	Lift height	0.05 m
System #2 Scotch-Yoke	J_{sy}	Combined Rotary inertia (motor + disk)	0.09 kg-m^2
	M_y	Yoke mass	0.8 kg
	s_2	Yoke displacement	-
	θ_{sy}	Disk angular displacement	-
	ω_{sy}	Disk angular speed	-
	r	Pin distance from centre	0.06 m

For the cam-follower & scotch–yoke configuration, a similar synchronization pattern governed by resonance is observed, even though the two mechanisms are fundamentally different. As shown in Fig. 9 for the 45 V – 59 V input case, both subsystems settle at a common steady state sync speed of 87 rad/s which is closer to the system's natural frequency (Ω_1 = 100 rad/s). This suggests that the overall dynamic behavior remains consistent, with resonance playing an important role in synchronization within the system. The intermediate block experiences sustained large-amplitude oscillations, which enhance the transfer of energy between the subsystems and eventually lead to in-phase synchronization. Even though the two mechanisms are structurally asymmetric, strong coordination is still achieved within the primary resonance region.

(a)

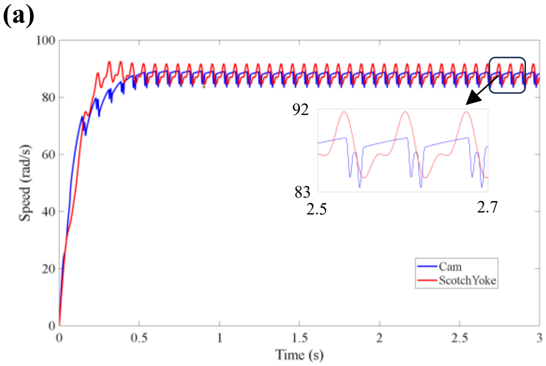

(b)

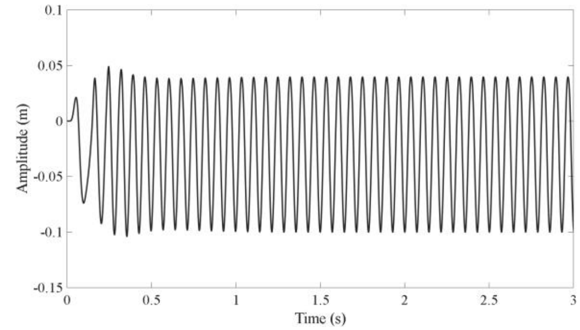

FIG. 9. IN-PHASE SYNC AT $V_1 = 45\ V, V_2 = 59\ V$, (a) SPEED RESPONSE OF CAM & SCOTCH-YOKE, (b) DISPLACEMENT OF BLOCK MASS

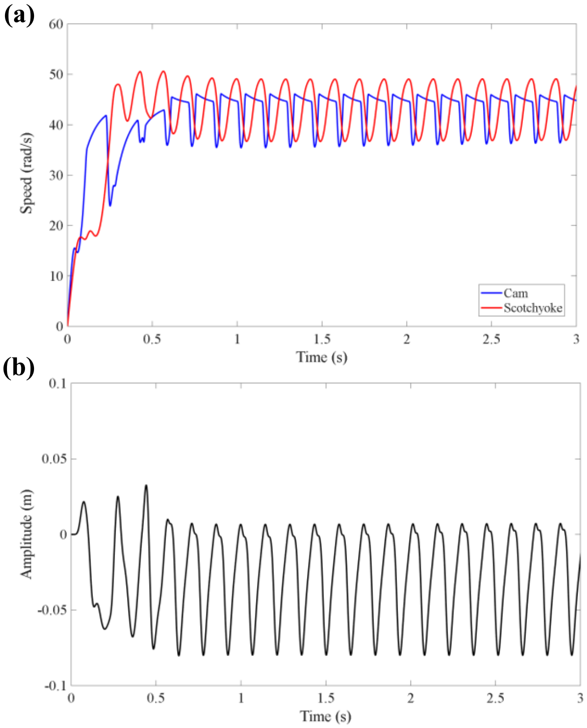

FIG. 10. IN-PHASE SYNC AT $V_1 = 22\ V, V_2 = 26\ V$, (a) SPEED RESPONSE OF CAM & SCOTCH-YOKE, (b) DISPLACEMENT OF BLOCK MASS

At lower voltage input combinations of 22 V and 26 V, as shown in Fig. 10, synchronization is observed near the subharmonic corresponding to half of the natural frequency (i.e., Ω_1 / 2 = 50 rad/s). The corresponding sync speed is 45 rad/s. This behaviour is similar to that observed in the cam–cam configuration, where subharmonic resonance resulted in weaker but still noticeable synchronization. In this case, the smaller oscillation amplitude of the intermediate block suggests weaker coupling between the two subsystems, although in-phase motion is still present. Overall, even for dissimilar mechanisms, both the primary and subharmonic resonance regions play a dominant role in enabling resonance locking and the emergence of synchronized behavior.

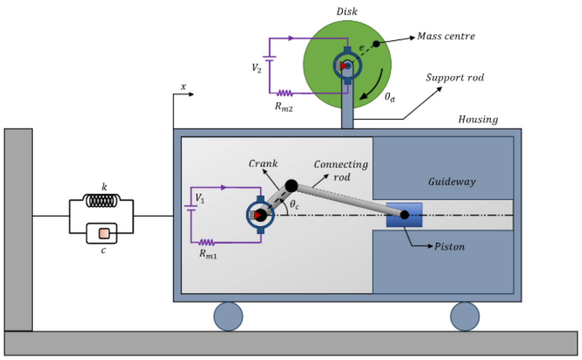

FIG. 11. SCHEMATIC OF ACTIVE EXCITATION MODEL (CASE II) OF A VIBRATING STRUCTURE SHARED BY SLIDER CRANK MECHANISM (SCM) & ECCENTRIC DISK ROTOR (EDR) SYSTEMS

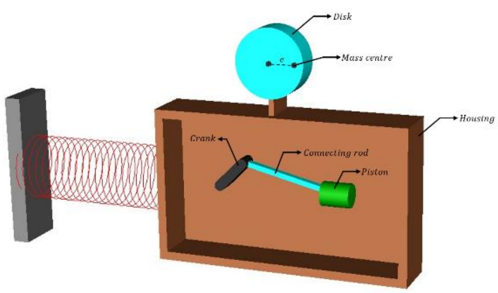

FIG. 12. ADAMS MODEL OF THE ACTIVELY EXCITED SCM-EDR SETUP (CASE II) – (DC MOTOR DRIVE AND DAMPER NOT SHOWN)

4. Case II - ACTIVE EXCITATION MODEL

After looking at the base-excited, passively coupled configurations, the focus has now moved on to actively excited models. In these models, the source of interaction comes from the dynamics of the subsystems themselves, not from imposed base motions.

In the setup for Case II (see Fig. 2), the interaction happens through a vibrating base structure that directly holds two mechanisms that can be driven independently. In this case, system #1 is a slider–crank mechanism (SCM) that is powered by a motor, and system #2 is an eccentric disk rotor (EDR). Both subsystems are attached to the same housing, which causes the excitation to come from their natural dynamic unbalances (see Fig. 11). The SCM adds a mix of reciprocating and rotating unbalances, while the EDR only adds rotational imbalance. Together, these create a coupled forcing environment in the shared structure.

It is important to note that the eccentric disk rotor is modeled as a rigid body with a fixed mass eccentricity, which means that it only creates a centrifugal unbalance force when it spins. This force is thought to act like a single-frequency harmonic excitation that is fully transmitted to the housing through a rigid mount.

In this setup, the vibrating base itself serves as the medium of interaction. It responds to and redistributes the forces created by the two subsystems. The coupling is force-driven because the motor-driven unbalances continue to send energy into the system. Table 3 shows a summary of the nomenclature and parameters for the whole system. Fig. 12 shows the corresponding multi-body dynamics model that was created in MSC Adams.

Table 3. Nomenclature and modelling parameters – Case II

Components	Symbol	Description	Value
Motor #1	V_1	Voltage supply	-
	k_{m1}	Characteristic constant	0.5 Nm/A
	R_{m1}	Circuit resistance	0.1 Ω
Motor #2	V_2	Voltage supply	-
	k_{m2}	Characteristic constant	0.5 Nm/A
	R_{m2}	Circuit resistance	0.1 Ω
System #1 Slider-crank mechanism (SCM)	J_c	Combined Rotary inertia (motor 1 & crank)	0.17 kg-m^2
	θ_c	Crank angular displacement	-
	ω_c	Crank angular speed	-
	m_c	Crank mass	1 kg
	m_{cr}	Connecting rod mass	2 kg
	m_p	Piston mass	4 kg
	J_{cr}	Connecting rod rotary inertia	0.0001 kgm^2
	l_c	Crank length	0.2 m
	l_{cr}	Connecting rod length	0.6 m
System #2 Eccentric disk-rotor (EDR)	J_d	Combined Rotary inertia (motor 2 & eccentric disk)	0.15 kg-m^2
	m_d	Disk mass	5 kg
	e	eccentricity	0.1 m
	θ_d	Disk angular displacement	-
	ω_d	Disk angular speed	-

	m_m	Mounting mass	1 kg
Miscellaneous	m_h	Housing Mass	12 kg
	x	Housing displacement	-
	M_{tot}	Total mass of whole assembly	25 kg
	k	Spring stiffness	250000 N/m
	c	Viscous damping	300 Ns/m
	Ω_2	Natural frequency of model (case II)	100 rad/s

After examining at the passively coupled configurations, the discussion now moves on to Case II, where the dynamic unbalances of the two mounted mechanisms directly excite the housing. In this setup, the slider-crank mechanism adds both rotating and reciprocating unbalances, while the eccentric disk rotor only adds rotating unbalance. So, the interaction is no longer mediated through forced base motion, but through direct forcing of the shared housing. This change in the way the system is excited, and makes its dynamic behavior qualitatively richer because it can now support both in-phase and anti-phase synchronization.

Figure 13 shows that when the coupled system is near resonance, the two mechanisms settle into an in-phase synchronized state. The synchronized speed (see Fig. 13(a)) is close to the housing's resonance frequency, which is about 100 rad/s. The housing response shows sustained oscillations with a strong, dominant primary harmonic. In this regime, the system arranges itself so that the forcing contributions work together to create large vibrations in the housing and a synchronized state that is in-phase. The transient phase provides insight into how this coordination is established. At first, the motor with lower input power tries to speed up, while the higher-power motor slows down due to increased load interaction. Through this mutual adjustment, both systems gradually move toward a common steady-state speed. In this case, with voltage levels of 55 V and 85 V, the agreed-upon synchronized speed stabilizes around 91 rad/s. This is close to the natural frequency, indicating resonance capture.

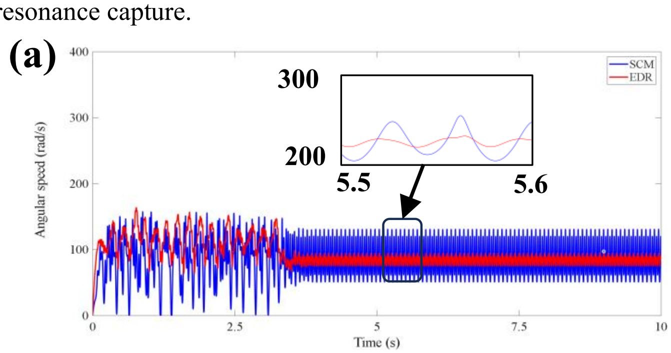

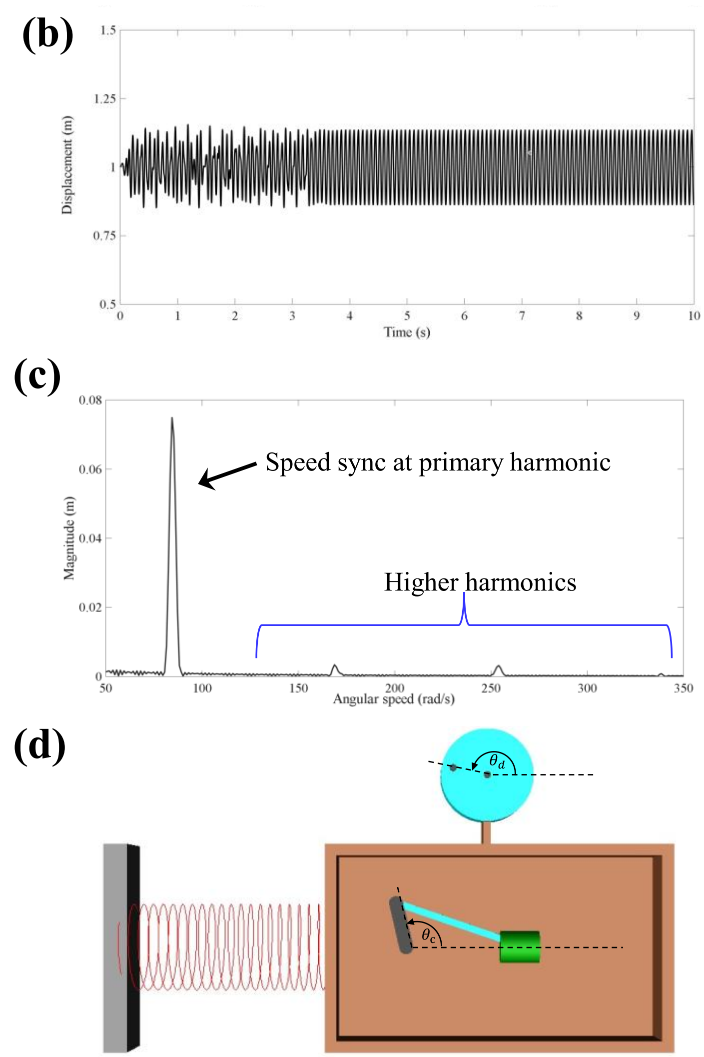

FIG. 13. IN-PHASE SYNC AT $V_1 = 55\,V, V_2 = 85\,V$, (a) SPEED RESPONSE OF SCM & EDR, (b) DISPLACEMENT OF HOUSING, (c) FFT OF HOUSING DISPLACEMENT RESPONSE AT STEADY STATE, (d) SCREENSHOT OF THE ADAMS ANIMATION FOR IN-PHASE SYNC VISUALIZATION

This convergence is also evident in the housing response (Fig. 13(b)). During the transient phase, the displacement shows a mixed and irregular oscillation pattern, revealing competing dynamic forces. As the system approaches steady state, the response shifts to a large-amplitude oscillation that is nearly harmonic. This indicates that the system has entered a resonance-dominated state.

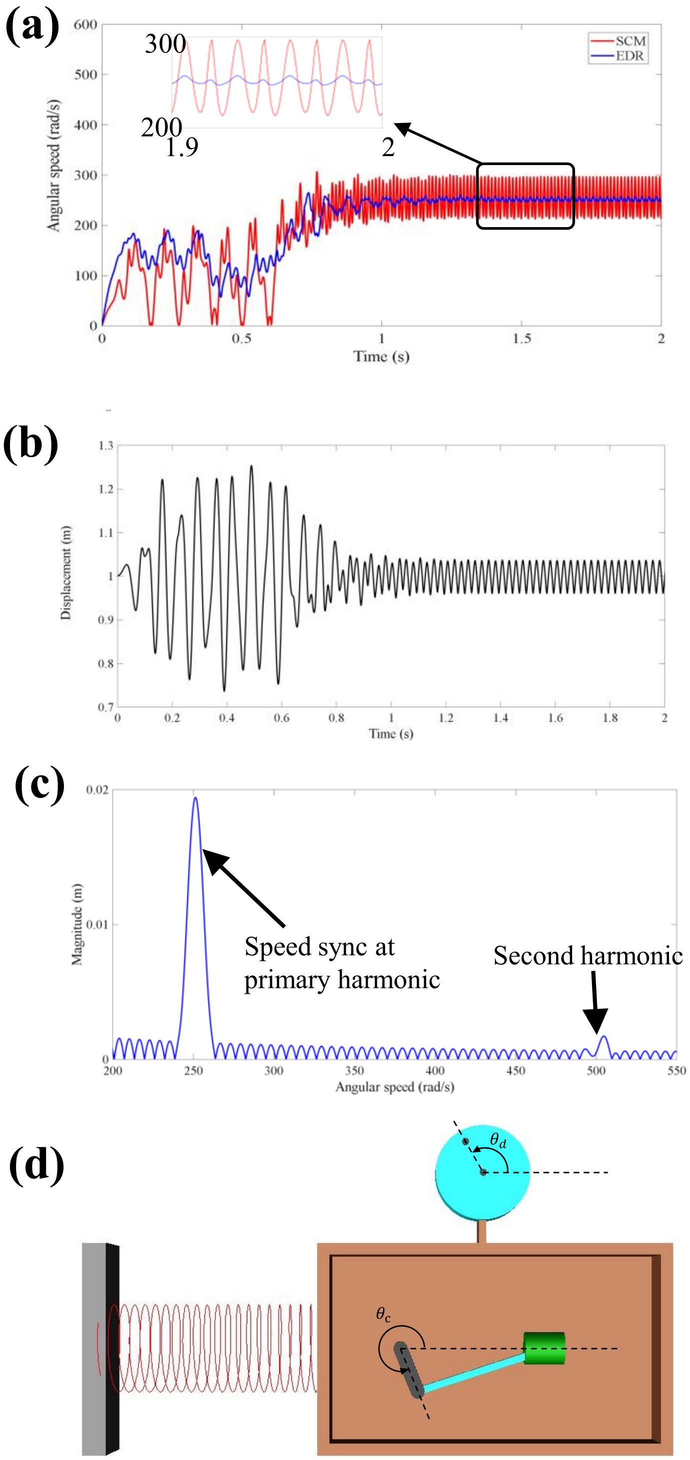

FIG. 14. ANTI-PHASE SYNC AT $V_1 = 120\,V, V_2 = 141\,V$, (a) SPEED RESPONSE OF SCM & EDR, (b) DISPLACEMENT OF HOUSING, (c) FFT OF HOUSING DISPLACEMENT RESPONSE AT STEADY STATE, (d) SCREENSHOT OF THE ADAMS ANIMATION FOR ANTI-PHASE SYNC VISUALIZATION

The FFT spectrum in Fig. 13(c) supports this further by showing a strong peak at 91 rad/s, corresponding to the synchronized motor speeds. There are also higher harmonics, which are mostly caused by the kinematic nonlinearity of the slider-crank mechanism. Their relative influence is governed by the obliquity ratio $n = l_{cr}/l_c$ for the SCM; lower values of n amplify higher harmonic content, while higher values suppress it. For the present case, with $n = 3$, the higher harmonics are present but remain secondary. The screenshot from the Adams simulation in Fig. 13(d) clearly shows this in-phase self-organization by showing the EDR and SCM's angular positions at steady state.

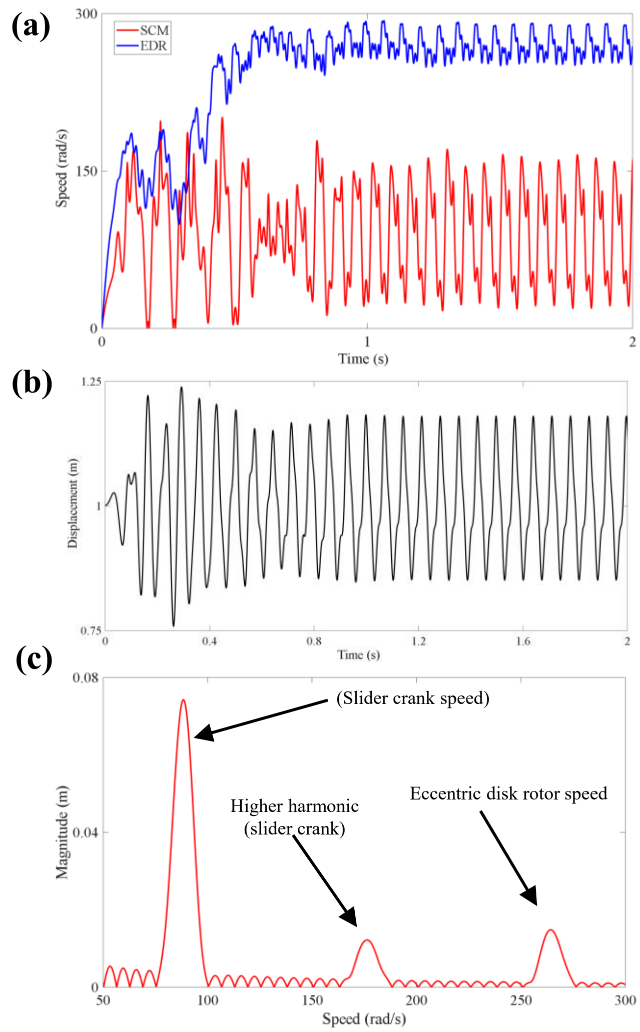

FIG. 15. DE-SYNC AT $V_1 = 120\,V, V_2 = 142\,V$, (a) SPEED RESPONSE OF SCM & EDR, (b) DISPLACEMENT OF HOUSING, (c) FFT OF DISPLACEMENT RESPONSE AT STEADY STATE.

Fig. 14 shows how the system behaves after it has left the resonance zone for a voltage combination of 120 V and 141 V. This is different from the behavior shown in Fig. 13. This causes anti-phase synchronization to happen. During the transient phase, the two mechanisms first show competing speed changes as they speed up past the resonance region. The motor with less input tends to speed up, while the motor with more power slows down because of more load interaction. This leads to convergence. Based on the motor's characteristics, the steady-state speeds for 120 V and 141 V should be about 240 rad/s and 282 rad/s, respectively. But the synchronized speed settles at an average of about 261 rad/s, which is close to the average of the two speeds. This averaged convergence is a typical feature of the post-resonance regime, where neither motor is in charge and the system finds a working point that works for both motors.

This behavior is also observed in the housing response and the contents of its spectrum. In the low-speed range, the transient vibrations are quite large, but once the system reaches steady state, the displacement amplitude drops a lot. This means that the system rearranges itself into an anti-phase configuration, which effectively reduces the overall structural vibration. The FFT spectrum in Fig. 14(c) shows a strong peak at this synchronized frequency (≈ 261 rad/s), which means that both subsystems have locked onto this common operating speed. There are higher harmonics again, but they don't have much of an effect because the SCM's obliquity ratio value is low. The Adams simulation snapshot in Fig. 14(d) supports this idea further by showing the SCM and EDR in anti-phase alignment at steady state. This indicates that once the system exceeds resonance, it rearranges itself to lessen structural excitation. With two interacting subsystems, this naturally leads to an approximate 180° phase separation, where their dynamic actions counter each other, resulting in reduced net vibration of the housing.

It is important to highlight that the phase adjustment process defines synchronization and cooperative dynamics in the system. Near resonance, the subsystems become in-phase to increase vibration energy. However, away from resonance, they shift their alignment to an anti-phase of around 180 degrees to decrease it. This self-alignment, governed by the underlying energetics, represents the basic organizing principle that drives the observed coordinated behavior [14].

In Figure 15, the desynchronization of the system under consideration is demonstrated for the 120 V and 142 V input configuration. It should be noted that only a slight change in the voltage of the second motor, from 141 V to 142 V (compare Figures 14 and 15), is needed for this transition from the anti-phase synchronized state to occur. The difference between the energy levels of two motors is too great to sustain the synchronized mode. While the weaker motor is still stuck in the resonance region, the stronger motor manages to escape to higher speeds and cannot achieve the same steady-state speed as the other motor (see Figure 15(a)). This leads to desynchronization and increased steady-state amplitude of the housing (Figure 15(b)).

The FFT response (Fig. 15(c)) further reflects this loss of coordination through the appearance of multiple distinct peaks rather than a single dominant frequency, corresponding to the separated motor speeds. This clearly demonstrates that once the power disparity exceeds a critical threshold, even the anti-phase synchronized state becomes unsustainable, leading to complete desynchronization.

4. CONCLUSION

Two distinct forms of vibrational interaction are examined as pathways to cooperative behavior in mechanical systems.

(1) Interaction through an intermediate vibrating structure, passively excited by base motions (cam–cam and cam–scotch–yoke systems) -

- *Exclusively in-phase response:* synchronization is strictly in-phase; anti-phase behavior is never observed.
- *Resonance-governed coordination*: synchronization only takes hold within resonance regimes, where large oscillations of the intermediate mass allow for meaningful energy exchange between the subsystems.
- *Loss of synchronization beyond resonance*: as the system moves away from resonance, the coupling fades and synchronization falls apart.
- *Sensitivity to power imbalance*: a large enough gap in input power is enough to break synchronization.
- *Persistence across subharmonic regimes*: in-phase synchronization can extend into subharmonic resonance zones, reinforcing the picture of strictly resonance-driven behavior.

(2) Interaction through a vibrating structure actively excited by reciprocating and rotating unbalances (slider–crank and eccentric rotor on a shared vibrating base):

- *Coexistence of dual modes:* in-phase and anti-phase synchronization both occur, offering a wider range of dynamic behavior.
- *Synchronization beyond resonance:* coordinated states survive outside of resonance. Resonance doesn't determine whether synchronization happens — it only shapes what kind occurs. In-phase motion tends to dominate near resonance, while anti-phase motion takes over as the system moves away from it.
- *Sensitivity to power imbalance:* a large mismatch in input power disrupts synchronization in both modes.

- *Self-organized dynamics:* the system naturally organizes itself. In-phase motion amplifies base vibrations, while anti-phase motion dampens them. This suggests the system settles into the configuration that best manages energy.
- *Greater tendency for synchronization:* active excitation injects sustained energy into the system. This strengthens the pull toward synchronization and expands the range of conditions under which it can happen. Overall, the potential for cooperative dynamics is much greater here than in the passive case.

Increasing damping primarily reduces the vibration amplitudes due to higher energy dissipation in the system. Consequently, the resonance-capture region associated with the Sommerfeld Effect becomes weaker, causing the system to escape resonance earlier. For Case I, this weakens the in-phase synchronization regime because the vibration-induced coupling between the motors is reduced. In Case II, increased damping decreases the in-phase synchronization region while increasing the possibility of anti-phase synchronization due to the earlier escape from resonance.

Taken together, the key takeaway is that the coordinated behavior observed in these systems is genuinely self-generated. It arises from internal energy exchange between the subsystems, with no need for external control, centralized coordination, or any imposed synchronization protocol. Understanding how this kind of self-organization works opens up interesting possibilities for designing distributed mechanical systems and cooperative machinery. Future work could explore adaptive control of synchronization states, extension to larger networks of mechanical agents, and applications in areas like vibration-assisted robotics, energy harvesting, and structurally integrated actuation platforms.

REFERENCES

[1] Nijmeijer, H., and Rodriguez-Angeles, A., Synchronization of Mechanical Systems, World Scientific Publishing, Singapore, 2003.
[2] Stefański, A., "Synchronization of Mechanical Systems Driven by Chaotic or Random Excitation," Journal of Sound and Vibration, 266(2), pp. 313–326, 2003.
[3] Zhang, X., Li, Z., Hu, W., and Wen, B., "Synchronization and Stability of a Nonlinear Vibrating Mechanical System Characterized by Asymmetrical Piecewise Linearity," Chinese Journal of Mechanical Engineering, 35(1), pp. 1–12, 2022.
[4] Zhang, X., Wen, B., and Zhao, C., "Theoretical, Numerical and Experimental Study on Synchronization of Three Identical Exciters in a Vibrating System," Chinese Journal of Mechanical Engineering, 26(3), pp. 1–10, 2013.
[5] Velayudhan, J., and Narayanan, M. D., "On the Synchronization Behavior of Coupled Friction-Induced Oscillators Subjected to Base Excitation," ASME Journal of Computational and Nonlinear Dynamics, 17(9), pp. 1–12, 2022.
[6] Mou, X., Xie, Z., Su, M., and Sun, B., "A Review of Theoretical Research on Synchronous Vibration of Excitation Devices," Journal of the Brazilian Society of Mechanical Sciences and Engineering, pp. 1–15, 2026.
[7] Sen, M., and López Cajún, C. S., "Review of Synchronization in Mechanical Systems," in Nonlinear Structural Dynamics and Damping, Springer, pp. 1–20, 2019.
[8] Majewski, T., "Vibratory Forces and Synchronization in Physical Systems," Ingeniería Mecánica, Tecnología y Desarrollo, 4(3), pp. 1–10, 2013.
[9] Blekhman, I. I., Synchronization in Science and Technology, ASME Press, New York, 1988.
[10] Blekhman, I. I., Vibrational Mechanics: Nonlinear Dynamic Effects, General Approach, Applications, World Scientific, Singapore, 1999.
[11] Fradkov, A. L., and Pogromsky, A. Y., Introduction to Control of Oscillations and Chaos, World Scientific, Singapore, 1998.
[12] Pikovsky, A., Rosenblum, M., and Kurths, J., Synchronization: A Universal Concept in Nonlinear Sciences, Cambridge University Press, 2001.
[13] Sinha, A., Bharti, S. K., Samantaray, A. K., and Bhattacharyya, R., "Sommerfeld Effect in a Single-DOF System with Base Excitation from Motor Driven Mechanism," Mechanism and Machine Theory, 2020.
[14] Sinha, A., Bharti, S. K., Samantaray, A. K., and Bhattacharyya, R., "Self-Synchronization in a Class of Motor Driven Reciprocating Mechanisms," Proceedings of the ASME International Mechanical Engineering Congress and Exposition (IMECE2019), 2019.

